Covalently Linked Ferrocenyl Quinones: Proton-Dependent Redox Behavior and Charge Redistribution

Stephen B. Colbran,* Sang Tae Lee, David G. Lonnon, Felicia J. D. Maharaj, Andrew M. McDonagh,† Katherine A. Walker, and Rowan D. Young

School of Chemistry, University of New South Wales, Sydney, NSW 2052, Australia

Received January 12, 2006

The proton-dependent redox chemistry of dyads comprised of a ferrocenyl electron donor directly linked to a hydroquinonyl electron donor or to a quinone electron acceptor by a single covalent bond has been characterized. Ferrocenyl-1,4-hydroquinone (**2**), ferrocenyl-1,4-benzoquinone (**3**), 3-ferrocenyl-1,2-catechol (**5**), and the precursors ferrocenyl-1,4-dimethoxybenzene (**1**) and 3-ferrocenyl-1,2-dimethoxybenzene (**4**) were studied; also the unstable compound 3-ferrocenyl-1,2-benzoquinone (**6**) was observed in the spectroelectrochemistry of **5**. Detailed cyclic voltammetry, coulommetry, and UV−vis−NIR spectroelectrochemistry experiments allied with EPR, NMR, and Mössbauer spectroscopy were used to probe the pH-dependent redox chemistry and electron distribution within the compounds.

Introduction

The archetypal reversible organometallic redox couple is perhaps the $Fe^{III}-Fe^{II}$ couple of ferrocene,[1,2] and the quinone−semiquinone−hydroquinone redox system[3,4] provides an exemplar for proton-dependent redox chemistry. It is little surprise, therefore, that dyads comprised of ferrocene electron donors indirectly tethered by amide,[5] ethynylene,[6−9] or vinylene[7,9,10] linkages to quinone acceptors have recently been targeted for investigation. Research involving these dyads has provided new insights into unusual structural and spin separation processes driven by proton-coupled intramolecular electron transfer[8−10] and has highlighted the role of hydrogen bonding and ion pairing on the stabilities and lifetimes of charge-separated states formed by thermal or photoinduced electron transfer within such dyads.[5] Species with proton-switchable fluorescence or nonlinear optical properties have been reported,[6,7] with other examples proposed as pH/metal ion-dependent photochromic switches for single-molecule electronic or sensor applications.[5,11] Ferrocenyl-quinones with a direct covalent bond between the ferrocene donor and (hydro)quinone (donor/)acceptors also have potential applications in homogeneous catalysis, antitumor therapeutics, and molecular electronic technologies.[9,12,13]

Despite all of the interest in ferrocenyl-(hydro)quinones, the redox chemistry of the directly linked systems has not been studied. In response, we have undertaken a detailed electrochemical and spectroelectrochemical investigation of the proton-dependent redox chemistry of the prototypal ferrocenyl-(hydro)-quinones, **1**−**6** (Chart 1).

Results and Discussion

Synthesis. The syntheses of **1**−**3** have been previously published by Kasahara et al., although this report is not widely available.[13] The synthesis of **1** involves coupling of the diazonium salt of 2,5-dimethoxyaniline to ferrocene under acidic conditions. After chromatographic purification, **1** was obtained in 25% yield. Cleavage of the methoxy substituents using boron tribromide yielded crude **2** as an oily yellow solid. Purification of **2** was achieved by first oxidizing with 2,3-dichloro-5,6-

* Corresponding author. E-mail: s.colbran@unsw.edu.au.

† Current address: School of Chemistry, Materials and Forensics, University of Technology Sydney, Sydney, NSW 2007, Australia.

(1) (a) Gagne, R. R.; Koval, C. A.; Lisensky, G. C. *Inorg. Chem.* **1980**, *19*, 2854−2855. (b) Connelly, N. G.; Geiger, W. E. *Chem. Rev.* **1996**, *96*, 877−910.

(2) Togni, A. *Ferrocenes*; VCH: New York, 1995.

(3) Gupta, N.; Linschitz, H. *J. Am. Chem. Soc.* **1997**, *119*, 6384−6391.

(4) (a) Bauscher, M.; Mantele, W. *J. Phys. Chem.* **1992**, *96*, 11101−11108. (b) Chambers, J. Q. Electrochemistry of Quinones. In *The Chemistry of the Quinonoid Compounds*; Rappoport, Z., Patai, Z., Eds.; J. Wiley & Sons: New York, 1988; Vol. II, Chapter 12, pp 719−757. (c) Laviron, E. *J. Electroanal. Chem.* **1986**, *208*, 357−372. (d) Eggins, B. R.; Chambers, J. Q. *J. Electrochem. Soc.* **1970**, *117*, 186−192.

(5) (a) Okamoto, K.; Fukuzumi, S. *J. Am. Chem. Soc.* **2004**, *126*, 13922−13923. (b) Fukuzumi, S.; Okamoto, K.; Yoshida, Y.; Imahori, H.; Araki, Y.; Ito, O. *J. Am. Chem. Soc.* **2003**, *125*, 1007−1013. (c) Moriuchi, T.; Shen, X. L.; Saito, K.; Bandoh, S.; Hirao, T. *Bull. Chem. Soc. Jpn.* **2003**, *76*, 595−599. (d) Fukuzumi, S.; Yoshida, Y.; Okamoto, K.; Imahori, H.; Araki, Y.; Ito, O. *J. Am. Chem. Soc.* **2002**, *124*, 6794−6795. (e) Fukuzumi, S.; Okamoto, K.; Imahori, H. *Angew. Chem., Int. Ed.* **2002**, *41*, 620−622.

(6) Butler, I. R.; Callabero, A. G.; Kelly, G. A.; Amey, J. R.; Kraemer, T.; Thomas, D. A.; Light, M. E.; Gelbrich, T.; Coles, S. J. *Tetrahedron Lett.* **2004**, *45*, 467−472. Rangel-Rojo, R.; Kimura, K.; Matsuda, H.; Mendez-Rojas, M. A.; Watson, W. H. *Opt. Commun.* **2003**, *228*, 181−186. McGale, E. M.; Murray, R. E.; McAdam, C. J.; Morgan, J. L.; Robinson, B. H.; Simpson, J. *Inorg. Chim. Acta* **2003**, *352*, 129−135.

(7) McGale, E. M.; Robinson, B. H.; Simpson, J. *Organometallics* **2003**, *22*, 931−939.

(8) (a) Murata, M.; Yamada, M.; Fujita, T.; Kojima, K.; Kurihara, M.; Kubo, K.; Kobayashi, Y.; Nishihara, H. *J. Am. Chem. Soc.* **2001**, *123*, 12903−12904. (b) Murata, M.; Fujita, T.; Yamada, M.; Kurihara, M.; Nishihara, H. *Chem. Lett.* **2000**, 1328−1329.

(9) (a) Murata, M.; Nishihara, H. *Macromol. Cont. Metal Metal-Like Elements* **2004**, *2*, 135−159. (b) Kurihara, M.; Nishihara, H. *Coord. Chem. Rev.* **2002**, *226*, 125−135. (c) Nishihara, H. *Adv. Inorg. Chem.* **2002**, *53*, 41−86.

(10) Kurihara, M.; Sano, H.; Murata, M.; Nishihara, H. *Inorg. Chem.* **2001**, *40*, 4−5.

(11) (a) Beer, P. D.; Crowe, D. B.; Ogden, M. I.; Drew, M. G. B.; Main, B. *J. Chem. Soc., Dalton Trans.* **1993**, 2107−2116. (b) Wagner, R. W.; Brown, P. A.; Johnson, T. E.; Lindsey, J. S. *J. Chem. Soc., Chem. Commun.* **1991**, 1463−1466. (c) Beer, P. D.; Kurek, S. S. *J Organomet. Chem.* **1989**, *366*, C6−C8.

(12) (a) Mathur, P.; Bhunia, A. K.; Mobin, S. M.; Singh, V. K.; Srinivasu, C. *Organometallics* **2004**, *23*, 3694−3700. (b) Cotton, H. K.; Huerta, F. F.; Bäckvall, J.-E. *Eur. J. Org. Chem.* **2003**, 2756−2763. (c) Zora, M.; Yucel, B.; Acikalin, S. *Tetrahedron Lett.* **2003**, *44*, 2237−2241. Chan, K. S.; Zhang, H. C. *Synth. Commun.* **1995**, *25*, 635−639. (d) Kasahara, A.; Shimizu, I.; Ookura, K. *Chem. Ind. (London)* **1986**, *8*, 285.

(13) Kasahara, A.; Izumi, T.; Ogata, H.; Tanno, S.; Fujisawa, T.; Ogata, T. *Bull. Yamagata Univ.* **1985**, *18*, 125−141.

10.1021/om060040x CCC: $33.50
Publication on Web 03/25/2006

Chart 1. Ferrocenyl-(hydro)quinones Investigated in This Work

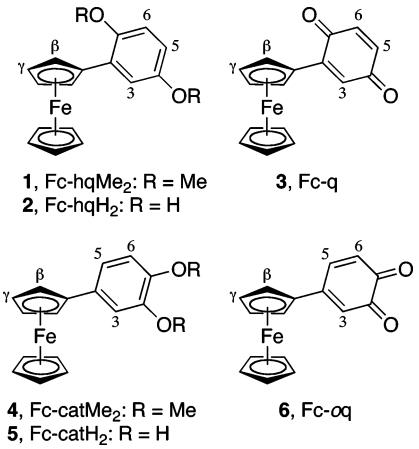

1, Fc-hqMe$_2$: R = Me
2, Fc-hqH$_2$: R = H
3, Fc-q

4, Fc-catMe$_2$: R = Me
5, Fc-catH$_2$: R = H
6, Fc-*o*q

Table 1. UV−Vis Data for 1−5 in Acetonitrile

	λ_{max}, nm (ϵ_{max}, cm^{-1} M^{-1})		
1	276 (6870),	314 (6450),	446 (325)
2	270 (6170),	309 (6150),	444 (280)
3	268 (6250),	393 (3040),	713 (1640)
4	242 (4190),	284 (3490),	445 (120)
5	241 (4380),	280 (3680),	452 (190)

dicyano-1,4-benzoquinone (DDQ) to give **3** as dark green microcrystals in 57% yield after recrystallization from hexanes. Reduction of **3** in dichloromethane with aqueous sodium dithionite afforded a clean sample of **2**.

Cleavage of the methyl substituents from previously reported[14] **4** using boron tribromide afforded the ferrocenylcatechol **5**. This new compound was difficult to isolate, as it decomposed rapidly in air, and more slowly on storage under an inert atmosphere at −15 °C, to intractable material that showed no evidence for a ferrocene moiety. Attempts to synthesize *ortho*-quinonylferrocene (**6**) by oxidation of **5** with oxidants such as silver oxide, DDQ, and phenyliodoso(diacetate) resulted only in decomposition. The instability of **5** (and **6**) may relate to the ability of the catecholate chelate ligand to strip iron from ferrocenes.[15]

Electronic, Mössbauer, and NMR Spectroscopy. Representative UV−vis−NIR spectra, those of **2** and **3**, are shown in Figure 1. The spectra of **1**, **2**, **4**, and **5** are all very similar, while the spectrum of **3** is significantly different (see Table 1 and Figure 1). The spectra of **1**, **2**, **4**, and **5** are typical of those for aryl-ferrocene derivatives; the bands at ca. 240−320 and at 445 nm are attributed to Fe (e_{2g}) → Cp (e_{1g}) charge-transfer and symmetry-forbidden Fe (a_{1g}) → Fe (e_{1g}) transitions, respectively.[16−18] These bands are more intense in ferrocenes with electron-withdrawing (e.g., aryl) substituents. In contrast, the spectrum of **3** is dominated by an intense band at 260 nm, which is typical of quinone (n, $\pi \rightarrow \pi^*$) transitions,[19] and a very strong band at 395 nm and a strong, broad band at 713 nm, neither of which are observed in the spectra of the other ferrocenes nor in the spectra of benzoquinones. The lower energy band at ∼713 nm is solvatochromic, whereas the 395 nm band shows little change in energy with solvent. The lower energy band distinctly trends to higher energy in more highly solvating solvents (a plot of band wavelength against Reichardt's "overall solvation scale" parameter, $E_T(30)$,[20] is given as Supporting Information). Accordingly, this band is attributed to an intramolecular charge-transfer transition between the ferrocenyl donor and quinonyl acceptor centers [e_π(HOMO-Fc) → e_π*(LUMO-q)]. The assignment is analogous to that of the well-characterized ferrocene-acceptor charge-transfer bands[16,21,22] such as the ferrocene e_π(HOMO) → DDQ e_π*(LUMO) charge-transfer band[22] and concurs with the disappearance of the band upon one-electron oxidation of the ferrocene center or one-electron reduction of the quinone center (discussed below).

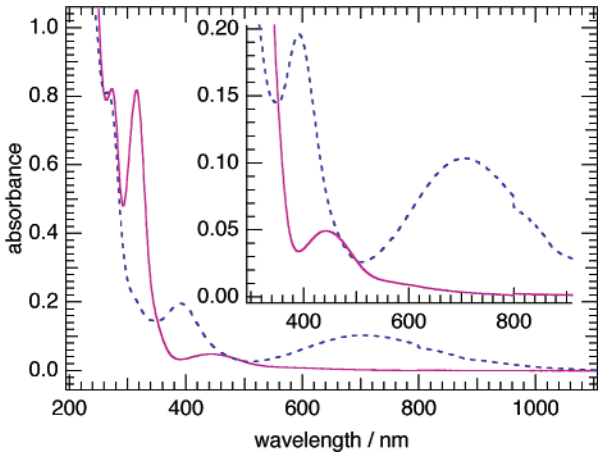

Figure 1. UV−vis−NIR spectra of **2** (solid trace) and **3** (dashed trace) in acetonitrile at 298 K.

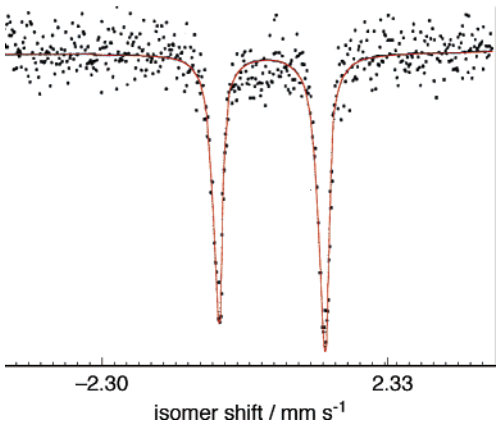

Figure 2. Zero-field ^{57}Fe Mössbauer spectrum of Fc−q at 298 K.

The zero-field ^{57}Fe Mössbauer spectrum of **3**, Figure 2, reveals a typical ferrocene doublet; the isomer shift is 0.43 ± 0.01 mm s^{-1} and the quadrupole splitting is 2.20 ± 0.01 mm s^{-1}. Under identical conditions, the measured values for ferrocene were 0.44 and 2.38 mm s^{-1}, respectively. The pronounced reduction in the quadrupole splitting for **3** compared to ferrocene[16,23] indicates net ground-state charge transfer from

(14) Beer, P. D.; Sikanyika, H.; Blackburn, C.; McAleer, J. F.; Drew, M. G. B. *J. Chem. Soc., Dalton Trans.* **1990**, 3295−3300.
(15) (a) Bashkin, J. K.; Kinlen, P. J. *Inorg. Chem.* **1990**, *29*, 4507−4509. (b) Prins, R.; Korswage, A. R.; Kortbeek, A. G. *J. Organomet. Chem.* **1972**, *39*, 335−344.
(16) (a) Barlow, S.; Bunting, H. E.; Ringham, C.; Green, J. C.; Bublitz, G. U.; Boxer, S. G.; Perry, J. W.; Marder, S. R. *J. Am. Chem. Soc.* **1999**, *121*, 3715−3723. (b) Barlow, S.; Ohare, D. *Chem. Rev.* **1997**, *97*, 637−669.
(17) (a) Gordon, K. R.; Warren, K. D. *Inorg. Chem.* **1997**, *17*, 9987−9995. (b) Dowben, P. A.; Driscoll, D. C.; Tate, R. S.; Boag, N. M. *Organometallics* **1988**, *7*, 305−308.
(18) Rosenblum, M.; Santer, J. O.; Howells, W. G. *J. Am. Chem. Soc.* **1962**, *85*, 1450−1456.
(19) Itoh, T. *Chem. Rev.* **1995**, *95*, 2351−2368.
(20) Reichardt, C. *Chem. Rev.* **1994**, *94*, 2319−2358.
(21) Miller, J. S.; Epstein, A. J.; Reiff, W. M. *Chem. Rev.* **1988**, *88*, 201−220.
(22) Gebert, E.; Reis, A. H., Jr.; Miller, J. S.; Rommelmann, H.; Epstein, A. J. *J. Am. Chem. Soc.* **1982**, *104*, 4403−4410.

Table 2. Potential Data for Redox Processes from Cyclic Voltammetry[a]

compound	$E_{1/2}(Fe^{III}-Fe^{II})$/V	E_p(aryl or quinone centered)/V
1	−0.04[b]	+0.95[d]
2	−0.07[b]	+0.54[d] (+0.09[d,e])
3	+0.17[b]	−0.92,[b] −1.49[c]
4	−0.06[b]	+0.91[d]
5	−0.03[b]	+1.11[d]

[a] In acetonitrile−0.1 M $[Bu^n_4N][PF_6]$ at 298 K; scan rate 100 mV s^{-1}. [b] Reversible process ($\Delta E_p = \Delta E_p(Fc^+-Fc) = 65$ mV; $i_p^{reverse}/i_p^{forward} = 1.0$). [c] Quasi-reversible process ($\Delta E_p = 90$ mV at $\nu = 100$ mV s^{-1} and increased with ν; $i_p^a/i_p^c \approx 1.0$). [d] Irreversible process (no peak for the couple in the return sweep). [e] Cathodic peak in the reverse sweep that arises from the irreversible oxidation process.

the ferrocenyl group to the quinone center, consistent with the above analysis of the UV−vis data.

The NMR data for **1**−**5** (see the Experimental Section) also concur with these conclusions. The ^{1}H NMR spectra of **1**, **2**, **4**, and **5** show pairs of triplets for H^β and H^γ (see Chart 1) at δ 4.3−4.4 and 4.5−4.8. These are downfield of the singlets assigned to the unsubstituted cyclopentadienyl ring at ca. δ 4.1, which is characteristic for ferrocenes with electron-withdrawing substituents.[2,18] In the spectrum of **3**, the cyclopentadienyl singlet again appears at δ 4.10, whereas the cyclopentadienyl triplets are significantly further downfield at δ 4.58 and 4.91, due to additional deshielding with the increased delocalization of electron density toward the quinone substituent. In the ^{13}C NMR spectrum of **3** the carbonyl carbon signals appear at δ 186.4 and 185.9 (cf. those for 1,4-benzoquinone at δ 187.06).

Electrochemistry and Spectroelectrochemistry. The electrochemical behavior of **1**−**5** was surveyed by cyclic voltammetry with that of **2**−**5** studied in more detail by UV−vis−NIR spectroelectrochemistry. Table 2 presents a summary of the potential data for the observed redox couples (relative to the Fc^+-Fc couple with $E_{1/2}(Fc^+-Fc) = 0$ V), and typical cyclic voltammograms, those for **2** and **3**, are shown in Figure 3. Cyclic voltammograms of **1**, **2**, **4**, and **5** each exhibit a fully reversible one-electron process at ca. −0.05 V in acetonitrile corresponding to the $Fe^{III}-Fe^{II}$ couple. The 240 mV shift to higher potential in the $Fe^{III}-Fe^{II}$ couple for **3** compared to that of **2** is indicative of electronic delocalization from the ferrocene to the quinone in accord with the aforementioned spectroscopic properties.

Redox processes centered on the aryl groups are observed for **1**, **2**, **3**, and **4**. Both **1** and **4** show an irreversible anodic process at ~ +1 V, which are assigned to oxidation of the dimethoxyphenyl groups to give the corresponding cation radicals, eq 1, a process that for simple poly(alkoxy)arenes is electrochemically and chemically reversible and occurs at ~ +1 V.[24] That the second oxidations for **1** and **4** are irreversible indicates that the open-shell di(radical) dication products, $Fc^+-hqMe_2^+$ and $Fc^+-catMe_2^+$, are unstable species that rapidly decompose.

$$Fc^+-ArMe_2 \rightleftarrows Fc^+-ArMe_2^+ + e^- \qquad (1)$$

In the cyclic voltammograms of **2** and **5**, the $Fe^{III}-Fe^{II}$ couple is followed by an anodic peak at ~ +0.6 V for **2** and ~ +0.9 V for **5**. This peak arises from two-electron oxidation of the hydroquinone or catechol group to the corresponding quinone, eq 2. The irreversibility of the $2e^-$, $2H^+$ oxidation in acetonitrile

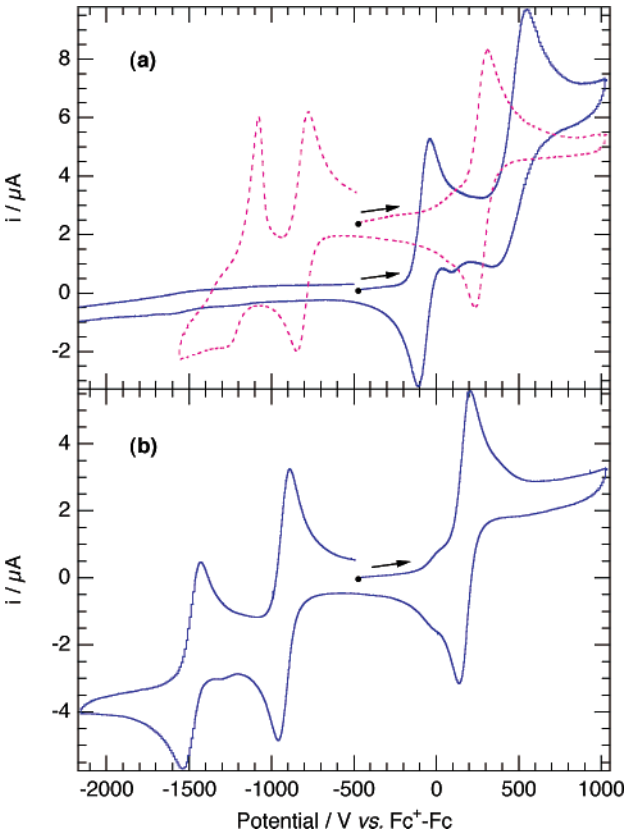

Figure 3. Cyclic voltammograms of (a) **2** (1 mM) before (solid trace) and after (dashed trace) addition of 3.0 equiv of $KOBu^t$ and (b) **3** (1 mM). Conditions: acetonitrile−0.1 M $[Bu^n_4N][PF_6]$ at 298 K; 0.5 mm glassy carbon minidisk working electrode; scan rate 100 mV s^{-1}.

Table 3. Species Characterized by UV−Vis−NIR Spectroelectrochemistry[a]

species	parent complex	λ_{max}, nm (ϵ_{max}, cm^{-1} M^{-1})
Fc^+−q	**3**	259 (22 700), 340 (sh, 5150), 644 (480)
Fc−q (**3**)	**3**	268 (13 200), 393 (3185), 710 (1680)
$Fc-sq^-$	**3**	277 (11 460), 323 (10 500), 427 (5080), 448 (5140), 535 (br sh)
$Fc-hqH^-$	**3**	271 (9960), 317 (8110), 450 (br sh, 1020)
$Fc-hqH_2$ (**2**)	**3**	273 (9460), 314 (7525), 444 (580)
Fc^+-hqH_2	**2**	253 (17 800), 284 (16 000), 365 (4240), 431 (2140), 598 (490), 858 (620)
$Fc-catMe_2$ (**4**)	**4**	242 (4190), 284 (3490), 445 (120)
$Fc^+-catMe_2$	**4**	250 (4670), 272 (sh, 4090), 364 (1040), 442 (810), 585 (75), 920 (220).
$Fc-catH_2$ (**5**)	**5**	242 (4600), 280 (3680), 450 (190)
Fc^+-catH_2	**5**	245 (4570), 278 (3835), 362 (880), 442 (620), 605 (80), 730 (170)
Fc−*o*q (**6**)	**5**	250 (vs), 432 (s), 690 (w)

[a] In acetonitrile−0.2 M $[Bu^n_4N][PF_6]$; the listed extinction coefficients are estimated from the absorbance of the listed band relative to those in the spectrum of the corresponding parent compound.

arises from the proton dependence of the chemical steps.[3,4] The small cathodic peak at +0.1 V in the reverse sweep is more pronounced when the solution is buffered with acid (see below) and is attributed to reduction of the quinone (reverse eq 2). Notably the quinone-centered reduction occurs prior to reduction of the ferrocenium center.

$$Fc^+-ArH_2 \rightarrow Fc^+-(o)q + 2H^+ + 2e^- \qquad (2)$$

Complex **3** also exhibits successive one-electron reductions of the quinone substituent, first to the semiquinone radical anion

(23) Bagus, P. S.; Walgren, U. I.; Almlof, J. *J. Chem. Phys.* **1976**, *64*, 2324−2334.

(24) (a) Zweig, A.; Hodgson, W. G.; Jura, W. H. *J. Am. Chem. Soc.* **1964**, *86*, 4124−4129. (b) Le Berre, V.; Angely, L.; Simonet, G.; Mousset, G.; Bellec, M. *J. Electroanal. Chem.* **1987**, *218*, 273−279.

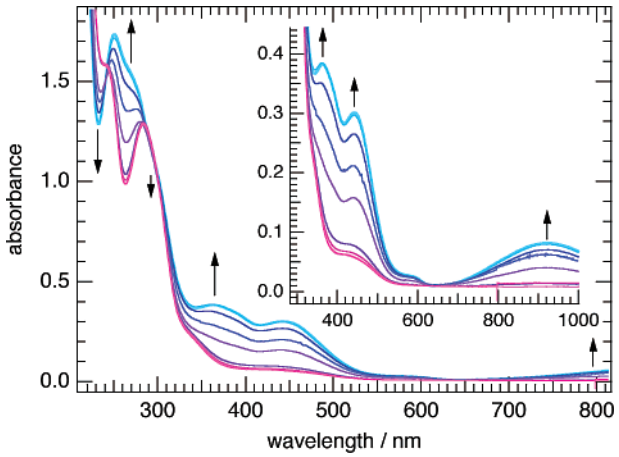

Figure 4. UV−vis spectroelectrochemistry for controlled-potential oxidation of **4** in acetonitrile−0.2 M [*n*-Bu_4N][PF_6] at 298 K at +0.5 V (vs Fc^+−Fc). Arrows mark the direction of absorbance change.

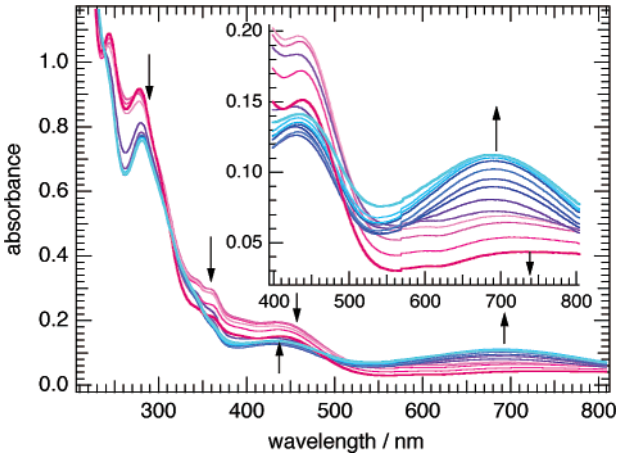

Figure 5. UV−vis−NIR spectroelectrochemistry for controlled-potential reduction $\mathbf{5}^+$ at −480 mV (vs Fc^+−Fc) showing the development of the strong charge-transfer band attributed to **6** at 690 nm (inset). The solvent is acetonitrile−0.2 M [Bu^n_4N][PF_6] at 298 K.

(at −0.92 V), eq 3, and then to the hydroquinone dianion, eq 4 (a quasi-reversible process at $E_{1/2} = -1.49$ V: $\Delta E_p \approx 100$ mV at scan rate 100 mV s^{-1}, cf. $\Delta E_p(Fc^+-Fc) = 65$ mV). In comparison, under identical conditions 1,4-benzoquinone is also reduced in two steps,[3,4] first forming the semiquinone anion (at $E_{1/2} = -1.09$ V) and then the hydroquinonyl dianion (at $E_{1/2} = -1.77$ V).

$$Fc-q + e^- \rightleftarrows Fc-sq^- \quad (3)$$

$$Fc-sq^- + e^- \rightleftarrows Fc-hq^{2-} \quad (4)$$

UV−vis−NIR spectroelectrochemical experiments confirm these assignments of the redox processes and provide spectroscopic evidence for production of the unstable *ortho*-quinone complex **6**, which we could not obtain by chemical oxidation. Table 3 presents a summary of the UV−vis−NIR spectroscopic data for the species that were characterized in these experiments.

The UV−vis−NIR spectra of the one-electron oxidation products of **2**, **4**, and **5** were obtained from in situ UV−vis−NIR spectroelectrochemical experiments and are very similar. Figure 4 shows UV−vis−NIR spectra acquired from a representative experiment, the oxidation of **4** at an electrolysis potential of +0.5 V. As expected from the cyclic voltammetry,

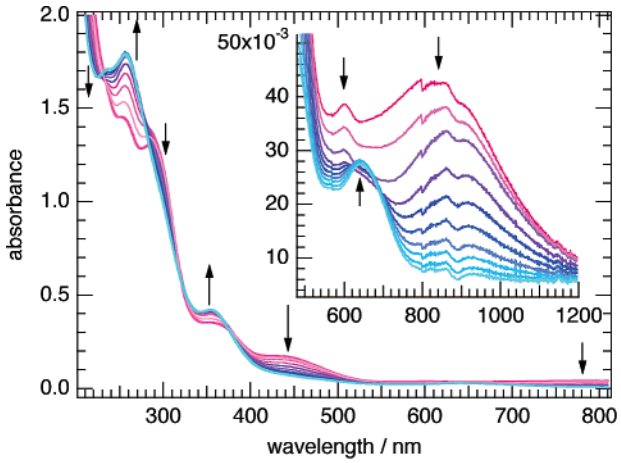

Figure 6. UV−vis−NIR spectroelectrochemistry for controlled-potential oxidation of $\mathbf{2}^+$ at +800 mV (vs Fc^+−Fc) in acetonitrile−0.2 M [Bu^n_4N][PF_6] at 298 K.

oxidation of the ferrocene center proceeds prior to aryl-centered oxidation as discussed above and affords the ferrocenium cation $\mathbf{4}^+$. The oxidation progressed with distinct isosbestic points at 243, 287, 302, and 650 nm until complete conversion of **4** into the oxidation product. Coulommetry revealed that the electrolysis consumed 0.97 F mol^{-1}. The oxidation was reversed by application of an electrolysis potential of −0.3 V. The electronic spectra of $\mathbf{2}^+$, $\mathbf{4}^+$, and $\mathbf{5}^+$ are all similar but unusual, as the distinctive lowest energy $^2e_{2g}$ (Fe) → $^2e_{1u}$ (C_5R_5) band for a ferrocenium ion at ∼600 nm[16−18] does not dominate the visible region. Rather, the electronic spectra are characterized by strong bands at ca. 370 and 450 nm, a very weak ferrocenium band at ca. 600 nm, and a broad band that extends into the NIR at ca. 920 nm for $\mathbf{4}^+$, at 840 nm for $\mathbf{2}^+$, and at 730 nm for $\mathbf{5}^+$ that are atypical of ferrocenes, ferrocenium cations, and (hydro)quinones. These spectra are very similar to those very recently reported by Robinson and co-workers for ethynyl-linked ferrocenium−polyaromatic dyads:[25] they attributed the lowest energy band to the characteristic[16,25] intervalent charge transfer from the electron-rich aryl group to the oxidizing ferrocenium centers, which in the present case would be Fc^+-ArR_2 → $\{Fc-ArR_2^+\}^*$ transitions, and used resonance Raman spectroscopy to reveal the bands at ∼370 and ∼440 nm to also have considerable intercenter charge-transfer character.

In unbuffered acetonitrile, the oxidations of **2** and **5** were not completely reversible; reduction of the cations $\mathbf{2}^+$ and $\mathbf{5}^+$ at −400 mV afforded the starting ferrocenyl-hydroquinone (**2** or **5**) contaminated by up to 20% of the corresponding ferrocenyl-quinone (**3** or **6**), e.g., Figure 5. The spectrum of **6** may be obtained by subtraction of that of **5** from that of the product mixture from reduction of $\mathbf{5}^+$. It has intense bands at 255 and 432 nm and a broad band in the visible region at 690 nm and is very similar to the spectrum of **3**.

The UV−vis−NIR spectroelectrochemical behavior during the second oxidation of **2** is shown in Figure 6. The bands assigned to Fc^+-hqH_2, $\mathbf{2}^+$, including the broad charge-transfer band at 850 nm, disappear as new bands at 260, 340, and 644 nm appear. The appearance of the 644 nm band is consistent with a ferrocenium center, and the 260 nm band is indicative for a quinone center,[19] suggesting the product is Fc^+-q, $\mathbf{3}^+$, in accord with the coulommetry, which revealed 1.8 F mol^{-1} were consumed, and with the cyclic voltammetry discussed above.

(25) Cuffe, L.; Hudson, R. D. A.; Gallagher, J. F.; Jennings, S.; McAdam, C. J.; Connelly, B. T. R.; Manning, A. R.; Robinson, B. H.; Simpson, J. *Organometallics* **2005**, *24*, 2051−2060.

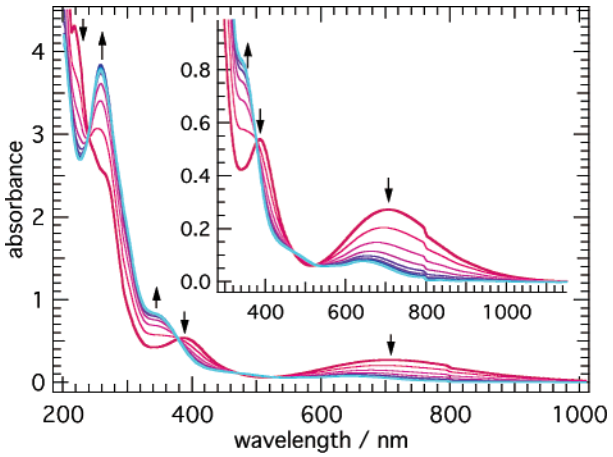

Figure 7. UV−vis-NIR spectroelectrochemistry for controlled-potential oxidation of **3** at +0.90 V (vs Fc^+−Fc) in acetonitrile−0.2 M [Bu^n_4N][PF_6] at 298 K.

Reduction of $\mathbf{3}^+$ at −400 mV cleanly produces the ferrocenyl-hydroquinone **2**. That reduction of the quinone group occurs in the present case and not for $\mathbf{3}^+$ produced by the oxidation of **3** (see below) is attributed to the stoichiometric production of protons during the oxidation of $\mathbf{2}^+$ according to eq 2. Thus, the pH in the solution is lowered and reduction of the quinone center occurs at higher potential[3,4] so that $\mathbf{3}^+$ is reduced to **2**.

Figure 7 reveals that the ferrocenium-quinone $\mathbf{3}^+$ is also cleanly produced by electrochemical oxidation of **3**. The spectrum is identical to that of the second oxidation product of **2**, Figure 6. Isosbestic points are observed at 239, 378, 472, and 526 nm, and all of the spectroscopic changes are fully reversed by electrolysis at +100 mV, which is consistent with a fully reversible oxidation process as predicted from the cyclic voltammetry of **3**. This highlights the role of the released protons (pH) during the reduction of $\mathbf{3}^+$ produced from oxidation of **2**. Noteworthily, chemical oxidation of **3** also gave $\mathbf{3}^+$. The UV−vis spectrum of the product from **3** and Ag[SbF_6] in tetrahydrofuran, after filtration to remove the precipitated Ag, was identical with that for $\mathbf{3}^+$ produced by electrolysis; however, **3**[SbF_6] tenaciously retained solvent and an analytically pure sample was not obtained.

Figure 8 depicts the spectroelectrochemical behavior of **3** at −1.0 V. This potential is poised just beyond the potential of the first reduction couple of **3**. The electrolysis was slow and incomplete due to the low overpotential; isosbestic points were observed at 285, 380, 406, and 620 nm, although the reduction was not fully reversible due to some slight decomposition of the reduction product. Arithmetic manipulation of the spectra (see Figure 8) reveals the reduction product has a band at 280 nm, as do all of the ferrocene derivatives reported in this work, plus bands at 326, 427, 448, 484 (sh), and 540 nm with the characteristic profile for a semiquinone (sq^-) radical anion.[26] This confirms the reduction product is Fc−sq^-, eq 3. Figure 9 shows the EPR spectrum of the Fc−sq^- radical. The spectrum shows a quartet at $g = 2.0056$ due to hyperfine coupling with the three protons of the semiquinonyl ring. The coupling at 0.227 mT is slightly, but significantly, lower than that of other semiquinone radicals, typically 0.241 mT,[27] indicative of delocalization of spin density from the now electron-rich semiquinone center onto the ferrocene.

(26) Okamoto, K.; Hirota, N.; Tominaga, T.; Terazima, M. *J. Phys. Chem. A* **2001**, *105*, 6586−6593.

(27) Fiedler, S. L.; Eloranta, J. *Magn. Reson. Chem.* **2005**, *43*, 231−234.

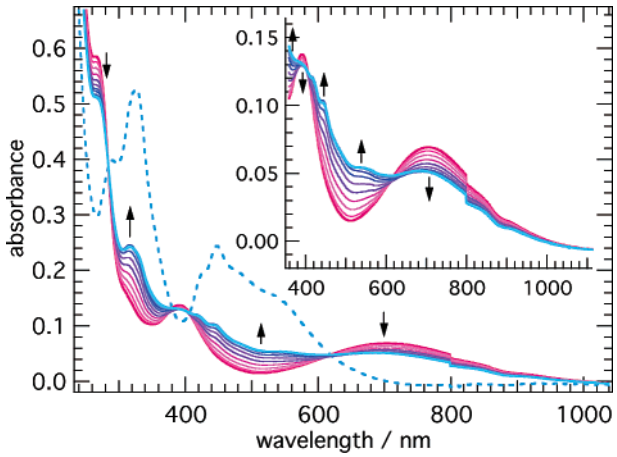

Figure 8. UV−vis−NIR spectroelectrochemistry for reduction of **3** at −1.0 V (vs Fc^+−Fc) in acetonitrile−0.2 M [Bu^n_4N][PF_6] at 298 K. The changes are (~85%) reversed by electrolysis at −0.15 V. The spectrum of the reduction product (dashed trace) was obtained by normalizing the first (**3**) spectrum and the final (reduction product + **3**) spectrum at 705 nm, subtracting the normalized first spectrum from the normalized final spectrum, and then scaling the absorbances so that they match those in all spectra at the isosbestic points.

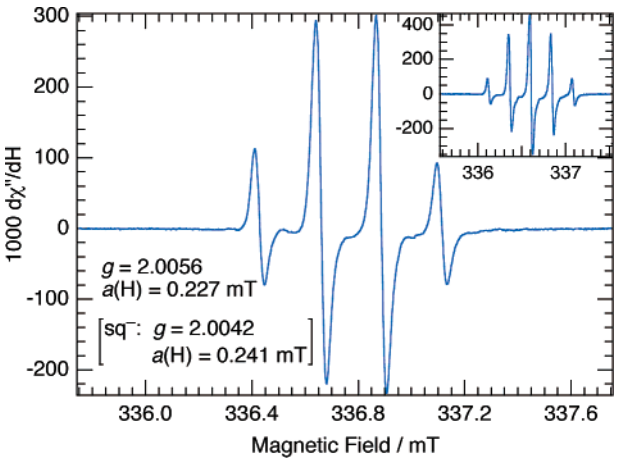

Figure 9. X-band EPR spectrum of Fc−sq^- obtained during in situ electrolysis of **3** at −1.0 V (vs Fc^+−Fc) in acetonitrile−0.1 M [Bu^n_4N][PF_6] at 298 K. Inset: X-band EPR spectrum of the semiquinone (sq^-) anion obtained from 1,4-benzoquinone under identical conditions.

Figure 10 shows the spectroelectrochemical behavior of **3** at the more reducing potential of −1.8 V. The first reduction process proceeded rapidly and was followed by a second process. The spectra in Figure 10a show the disappearance of the bands of **3** and the growth of the new bands for the semiquinone radical, Fc−sq^-. Figure 10b shows spectra obtained immediately following those shown in Figure 10a and corresponds to completion of the second reduction process. The resultant spectrum is quite similar to that of **2** and may be assigned to a ferrocene-hydroquinonyl species. This second reduction is not reversed upon electrolysis at −0.15 V. A plausible reason is that the basic hydroquinone dianion is unstable with respect to protonation under the neutral conditions employed and reacts to form the hydroquinonyl monoanion, Fc−hqH^-, eq 5 (*E*H = solvent or protic impurity, e.g., water). Overall, the reduction chemistry of Fc−q is thus described by eqs 3−5.

$$Fc{-}hq^{2-} + H{-}E \rightleftarrows Fc{-}hqH^- + E^- \qquad (5)$$

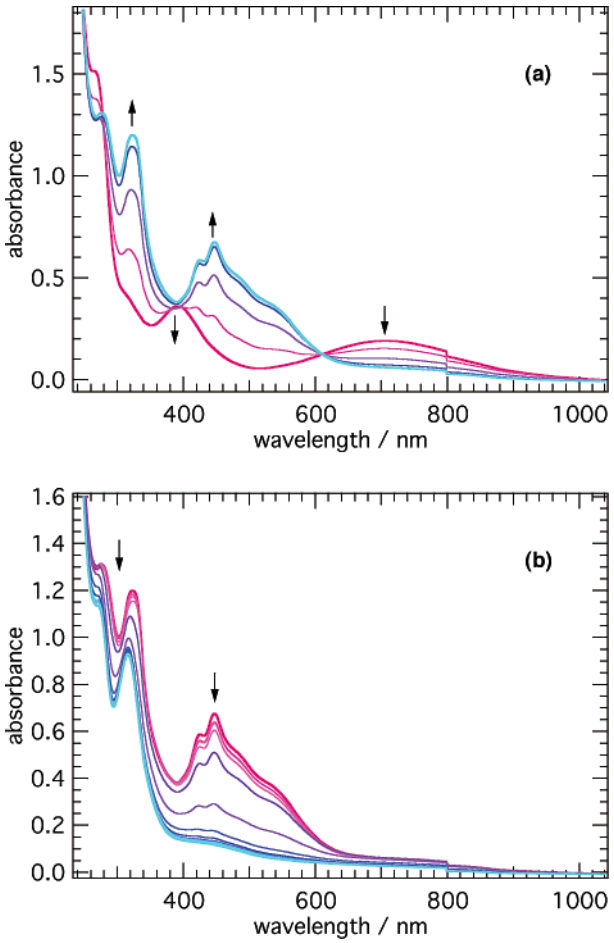

Figure 10. UV−vis−NIR spectroelectrochemistry for controlled-potential reduction of **3** at −1.8 V (vs Fc^+−Fc): (a) first six spectra; (b) subsequent spectra. Conditions: acetonitrile−0.2 M $[Bu^n_4N][PF_6]$ at 298 K; repetition time between spectra is 45 s.

Effect of Acid and Bases. The cyclic voltammograms of **2** and **3** were unaffected by the weak base 2,4,6-collidene (pK_a 7.3). Figure 3a shows a cyclic voltammogram of **2** before and after the addition of excess potassium *tert*-butoxide [pK_a 18, cf. pK_a(1,4-hydroquinone) 9.96]. The electrochemical behavior of **2** in the presence of the base is similar to that of **3**, Figure 3b, suggesting that the hydroquinonyl group is doubly deprotonated to afford the dianion, Fc−hq^{2-}, which is stable under these strongly basic conditions. This is consistent with the initial anodic current in the dotted trace in Figure 3a because Fc−hq^{2-} is spontaneously oxidized to Fc−q at the initial potential (−0.5 V). The behavior of the Fc−sq^-/Fc−hq^{2-} couple is suggestive of adsorption/precipitation of the potassium salt of the dianion on the working electrode. The distinct positive shifts in the Fc−q/Fc−sq^- and Fc−sq^-/Fc−hq^{2-} couples for the hydroquinone dianion Fc−hq^{2-}, Figure 3a, compared to the neutral quinone Fc−q, Figure 3b, result from the tighter anion−potassium counterion pairing[28] and anion−*tert*-butanol hydrogen bonding[3] associations caused by the presence of potassium ion and *tert*-butyl alcohol after reaction of **2** and potassium *tert*-butoxide.

Addition of weak acids did not affect the color or the UV−vis−NIR spectra of solutions containing **3**. Figure 11 shows cyclic voltammograms before and after addition of 2,4,6-collidinium triflate. Addition of collidinium triflate does not affect the ferrocene−ferrocenium couple, indicating that **3** is not protonated in solution in this case, consistent with the unperturbed electronic spectrum. However, the q−sq^- and sq^-−hq^{2-} couples are replaced by an irreversible, two-electron process at −0.54 V. This reveals the effect of weak acid on the stability of the semiquinone radical anion, which is rapidly protonated and disproportionates[3,4] according to eqs 6−8:

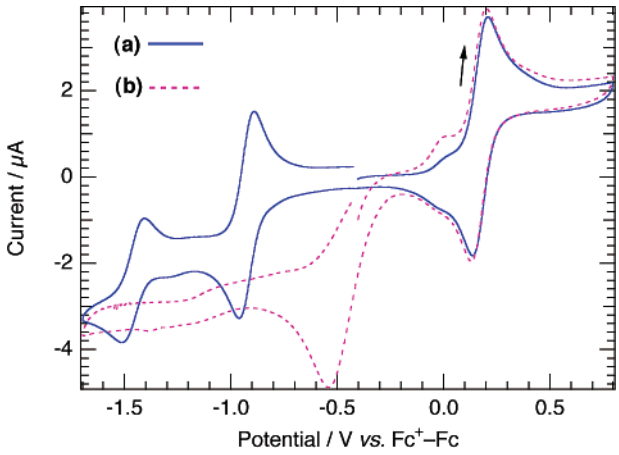

Figure 11. Cyclic voltammograms of **3** before (a) and after (b) addition of 2,4,6-collidinium triflate (2.0 equiv). Conditions: acetonitrile−0.1 M $[Bu^n_4N][PF_6]$ at 298 K, glassy carbon 0.5 mm minidisk working electrode, scan rate 100 mV s^{-1}.

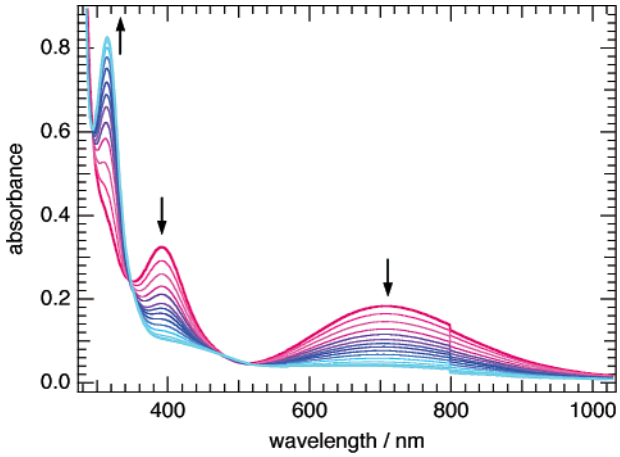

Figure 12. UV−vis−NIR spectroelectrochemistry for controlled-potential electrolysis of a solution containing **3** and excess 2,4,6-collidinium triflate (4.0 equiv) at −0.9 V (vs Fc^+−Fc) in acetonitrile−0.2 M $[Bu^n_4N][PF_6]$ at 298 K.

$$Fc{-}q + e^- \rightleftarrows Fc{-}sq^- \quad (6)$$

$$Fc{-}sq^- + H^+ \rightarrow Fc{-}sqH \quad (7)$$

$$2\ Fc{-}sqH \rightarrow Fc{-}q + Fc{-}hqH_2 \quad (8)$$

Since the disproportionation regenerates **3**, provided all steps are fast relative to the cyclic voltammetric (μs−ms) time scale, an overall two-electron reduction to the hydroquinone Fc−hqH_2 is observed. The proton dependence of the process renders it electrochemically irreversible.

Figure 12 shows the spectroelectrochemical behavior of **3** during reduction at −0.9 V in the presence of excess 2,4,6-collidinium triflate. As the electrolysis proceeds, the absorption bands of **3** are replaced by those for **2** (cf. Figure 1). Isosbestic

(28) LeSuer, R. J.; Geiger, W. E. *Angew. Chem., Int. Ed.* **2000**, *39*, 248−250.

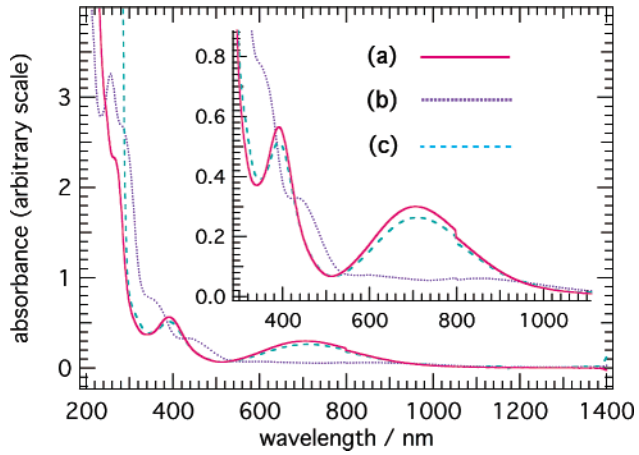

Figure 13. UV−vis−NIR spectra of (a) **3** in acetonitrile, (b) after adding excess aqueous 40% perchloric acid (0.1 mL into 10 mL of solution) to solution (a), and (c) after adding excess 2,4,6-collidine to solution (b). The spectra are not compensated for dilution effects; 2,4,6-collidene absorbs strongly below 300 nm.

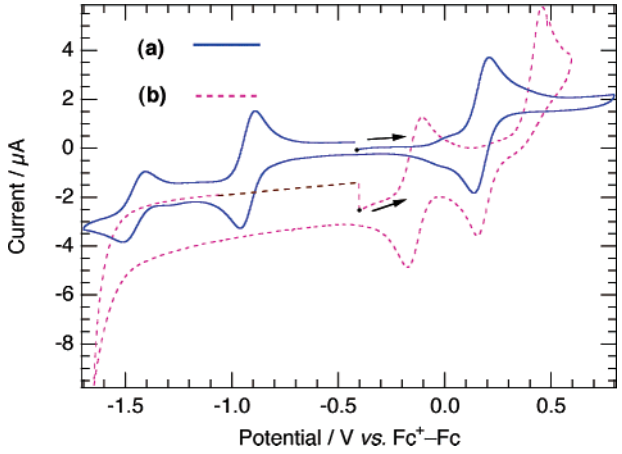

Figure 14. Cyclic voltammograms of **3** before (a) and after (b) addition of 40% aqueous perchloric acid (0.1 mL in 10 mL of solution). Conditions: acetonitrile−0.1 M $[Bu^n_4N][PF_6]$ at 298 K, glassy carbon 0.5 mm minidisk working electrode, scan rate 100 mV s^{-1}.

points at 297, 350, and 520 nm reveal this to be a clean transformation without accumulation of semiquinone intermediates.

In contrast, **3** exhibits quite different behavior upon addition of a strong acid. Addition of perchloric acid (pK_a −7) to solutions of **3** in acetonitrile caused an immediate color change from intense green to pale straw-yellow. In the corresponding UV−vis−NIR spectra, Figure 13, the intense charge-transfer band at 712 nm disappears and bands at 256, 354, and 640 nm for Fc^+−q (see above) plus bands at 296, 378, 441, 600, and 854 nm for Fc^+−hqH_2 (see above) appear. The change induced by the perchloric acid was completely reversed by neutralization with a weak base, e.g., collidine. The pK_a of 1,4-benzoquinone[3,4] is estimated to be −7, and the pK_a of the benzoquinonyl group in **3** will be raised by electron delocalization with the donor ferrocene. Therefore, the quinone group will be protonated at an oxygen after addition of perchloric acid, thereby raising its oxidation potential above that of the ferrocene center (see Figure 14 and the accompanying discussion below) and so inducing intramolecular electron transfer to produce the protonated semiquinone cation, Fc^+−sqH. As already mentioned, neutral (protonated) semiquinones are unstable with respect to disproportionation, which typically proceeds at close to diffusion-

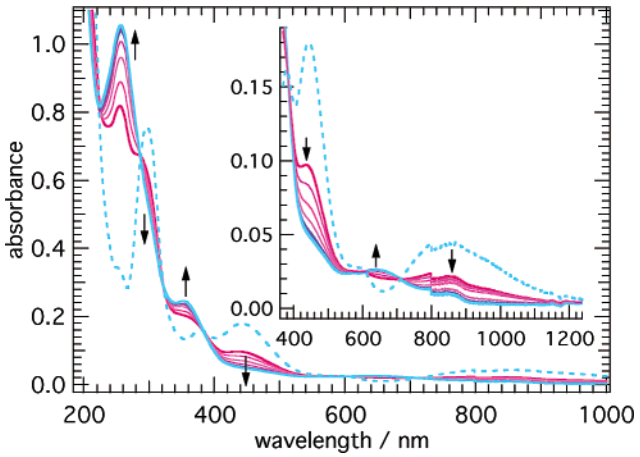

Figure 15. UV−vis−NIR spectroelectrochemistry for controlled-potential oxidation of **3** in the presence of excess aqueous perchloric acid (0.1 mL in 10 mL of solution) at +0.8 V (vs Fc^+−Fc) in acetonitrile−0.2 M $[Bu^n_4N][PF_6]$ at 298 K. (No change was observed when an electrolysis potential of +0.3 V was applied to the solution.) The dashed trace was obtained from the arithmetic manipulation, 2 × (*is* − 0.5*fs*), of the initial (*is*) and final (*fs*) spectra.

controlled rates.[3,4] The observation of bands for Fc^+−q and Fc^+−hqH_2 confirms that Fc^+−sqH disproportionates. Equations 9 and 10 thus summarize the response of **3** to strong acid.

$$Fc{-}q + H^+ \rightleftarrows Fc^+{-}sqH \qquad (9)$$

$$2\ Fc^+{-}sqH \rightleftarrows Fc^+{-}hqH_2 + Fc^+{-}q \qquad (10)$$

The cyclic voltammetry and UV−vis−NIR spectroelectrochemistry for **3** in the presence of excess perchloric acid is entirely consistent with internal electron transfer and disproportionation to afford a 1:1 mixture of Fc^+−hqH_2 and Fc^+−q ions. Addition of excess perchloric acid to **3** results in a cyclic voltammogram very similar to that of **2** but with the current cathodically displaced, Figure 14. The cathodic displacement of the initial current is indicative of spontaneous reduction of the ferrocenium and quinone centers in the 1:1 mixture of Fc^+−hqH_2 and Fc^+−q to afford **2** [or possibly Fc−hqH_3^+ (**2**H^+) in strong acid], which is the thermodynamically stable species in acid at the initially applied potential (−0.4 V). The observed Fe^{III}−Fe^{II} couple on adding the strong acid thus arises from **2**, not **3**, and accordingly is shifted to lower potential as discussed above. After acid is added, the anodic peak at +0.46 V corresponds to the 2e^-, 2H^+ oxidation of the hydroquinone group, eq 5, and the coupled cathodic peak at +0.18 V to the reverse process. In electrolysis, no current flowed and no change was observed when the electrolysis potential was set at +0.3 V (i.e., between the Fe^{III}−Fe^{II} couple and the potential for oxidation of the hydroquinone), consistent with only ferrocenium centers in the species in solution. Figure 15 shows the changes in the UV−vis−NIR spectrum upon electrolysis at +0.8 V, which consumed 0.97 F mol^{-1}; that is, overall it is a one-electron process. The bands for Fc^+−q at 256, 354, and 640 nm increase in intensity as those at 296, 378, 441, 600, and 854 for Fc^+−hqH_2 disappear; isosbestic points were observed at 223, 286, 322, 383, 608, and 709 nm for this clean transformation. The dotted trace in Figure 15 is the spectrum for Fc^+−hqH_2 obtained by subtraction of the spectrum of Fc^+−q (the final spectrum) from that of the 1:1 mixture of Fc^+−q and Fc^+−hqH_2 and corresponds to that obtained from direct oxidation of **2** at +0.3 V (see above).

Conclusion

The electrochemical behavior of the complexes investigated here is beyond that of the individual centers. The ferrocenyl-quinones **3** and **6** are deep brilliant green, the result of intense, solvatochromic ferrocene-donor to quinone-acceptor charge-transfer transitions in the visible region, which disappear upon one-electron reduction to Fc−sq$^-$ (**3**$^-$) or oxidation to Fc$^+$−q (**3**$^+$). Weaker intercenter charge-transfer transitions in the reverse direction are observed in the ferrocenium-acceptor, aryl-donor species **2**$^+$, **4**$^+$, and **5**$^+$.

In contrast to the results for ethynyl-linked ferrocene-quinone conjugates that suggest the centers are largely isolated in the ground state,[6,7,26] considerable delocalization of electron density from the donor ferrocene to acceptor quinone center is indicated by the physicochemical properties of **3**. The distribution of charge between the ferrocene and quinone centers of **3** is delicately balanced. Solutions of **3** become pale yellow after adding strong acid. In these low-pH solutions, the quinone group within **3** becomes a strong oxidant due to protonation at oxygen. This in turn leads to intramolecular electron transfer followed by disproportionation of the resulting semiquinone to afford a 1:1 mixture of Fc$^+$−hqH$_2$ and Fc$^+$−q cations. The reaction is completely reversed upon raising the pH of the solution.

We anticipate that these new insights into this archetypal redox system will facilitate progress in applications and redox-based devices. The new ferrocenyl-catechol **5** is potentially a redox-switchable chelate ligand to metal ions[29] and metal oxide surfaces.[30] Potential uses for the **2**−**3** system in molecular electronics applications are suggested by the range of accessible oxidation states, the redox-switchable low-energy charge-transfer transitions, and the pH-controlled switching from ferrocene-centered to (hydro)quinone-centered redox chemistry.

Experimental Section

General Comments. All reactions were performed under a nitrogen atmosphere in solvents dried and distilled using routine procedures. UV−vis−NIR spectra were recorded using a Cary 5 spectrophotometer. Solutions for electrochemistry and spectroelectrochemistry experiments were prepared in a nitrogen-filled Braun glovebox operating with water and oxygen levels both below 2 ppm; the compounds were ∼1.0 mM in anhydrous acetonitrile (Aldrich, used as received) with 0.1 or 0.2 M tetra-*n*-butylammonium hexafluorophosphate for cyclic voltammetry or spectroelectrochemistry and coulommetry experiments, respectively. Cyclic voltammetry measurements were performed in a conventional three-electrode cell using a computer-controlled Pine Instrument Co. AFCBP1 bipotentiostat as described in detail elsewhere.[31] The reported data are from cyclic voltammograms recorded with a 0.5 mm glassy carbon working electrode at a scan rate of 100 mV s^{-1}, and the potentials in this paper are quoted relative to the ferrocenium−ferrocene (Fe^{III}−Fe^{II}) couple measured under identical experimental conditions (same concentrations, solvent, support electrolyte, electrodes, temperature, and scan rate). The UV−vis−NIR spectroelectrochemical experiments were performed using a modified UV−vis−NIR cuvette with a Pt gauze working electrode, a Pt wire counter electrode, and an Ag/AgCl reference electrode. Coulommetry was performed in a conventional H-cell using Pt gauze working and ancillary electrodes and the same reference electrode as used in the cyclic voltammetry experiments; the stirred solvent−electrolyte solution in the working electrode compartment was exhaustively electrolyzed at the potential of interest prior to adding the compound for electrolysis, and the small residual current was subtracted from the integration of the current for the experiment. Infrared spectra were recorded using either a Perkin-Elmer 280B or Hitachi 260-10 instrument. High-resolution mass spectra (HR-MS) were obtained on a Bruker BioApex-II 7 T FT-ICR mass spectrometer, and low-resolution mass spectra were recorded using a VG Quattro mass spectrometer. Elemental microanalyses were carried out by the Microanalytical Service Unit at the Research School of Chemistry, Australian National University. Mössbauer spectra were recorded in transmission mode with a constant acceleration spectrometer at room temperature equipped with a ^{57}-Co/Pd source and a Wissel drive unit with associated Ortec electronics. The velocity scale was calibrated with metallic iron foil and sodium nitroferricyanide(III), and the isomer shift value quoted is relative to the midpoint of the iron spectrum at room temperature. The spectral parameters were extracted from least-squares fits of the data to Lorentzian line shapes.

Syntheses. Fc−hqMe$_2$ (1). The diazonium salt of 2,5-dimethoxyaniline was prepared by the slow addition of sodium nitrite (6.1 g, 0.10 mol) to a stirred solution of 2,5-dimethoxyaniline (12.24 g, 0.08 mol) in aqueous sulfuric acid (200 mL, 1 M). The resultant solution was added rapidly to ferrocene (18.6 g, 0.10 mol) dissolved in glacial acetic acid (900 mL) under an inert atmosphere. The resulting green/brown solution was stirred overnight at room temperature, and then poured into a saturated aqueous solution of sodium bisulfate (2000 mL). The mixture was extracted with dichloromethane (3 × 200 mL) and the combined organic extracts treated with aqueous sodium carbonate until neutral and then dried over magnesium sulfate. The solvent was removed and the product purified by silica column chromatography. Elution with dichloromethane/hexane (1:3) yielded 8.60 g (25%) of **1** as a red oil. HR-MS: *m*/*z* 322.06524 (calc M$^+$ ($C_{18}H_{18}FeO_2^+$) *m*/*z* 322.06507). ^{1}H NMR ($CDCl_3$): δ 7.13 (d, J_{HH} 3 Hz, $C_6H_3(OMe)_2$, 1 H), 6.82 (d, J_{HH} 9 Hz, $C_6H_3(OMe)_2$, 1 H), 6.74 (dd, J_{HH} 3, 9 Hz, $C_6H_3(OMe)_2$, 1H), 4.79 (t, C_5H_4, 2 H), 4.31 (t, C_5H_4, 2 H), 4.08 (s, C_5H_4, 5 H), 3.84 (s, CH_3, 3H), 3.82 (s, CH_3, 3H). ^{13}C NMR ($CDCl_3$): δ 153.3, 151.1, 128.5, 115.2, 112.1, 111.0, 82.5, 69.4, 69.9, 69.3, 55.6, 55.5. LR-MS: 323 (M$^+$ + 1, 23%), 322 (M$^+$, 100), 307 (M$^+$ − CH_3, 26), 292 (M$^+$ − 2CH_3, 73), 227 (M$^+$ − (2CH_3 + C_5H_5), 39). IR (neat (cm^{-1})): 3097 (w), 2999 (w), 2953 (m), 2940 (m), 2908 (w), 2836 (s), 1614 (m), 1513 (vs), 1473 (vs), 1441 (s), 1415 (w), 1393 (w), 1311 (m), 1291 (s), 1271 (s), 1236 (vs), 1221 (vs), 1030 (s), 1005 (m), 820 (s), 737 (m), 504 (s).

Fc−hqH$_2$ (2). Compound **3** (0.50 g, 1.7 mmol) was dissolved in dichloromethane and added to a separating funnel containing saturated aqueous sodium dithionite (100 mL). The mixture was shaken until the green dichloromethane layer became completely orange. The dichloromethane layer was washed with water and dried over anhydrous magnesium sulfate, and the solvent was removed in vacuo. Compound **2** was recovered as an orange solid (0.50 g, 99%). HR-MS: *m*/*z* 294.03386 (calc M$^+$ ($C_{16}H_{14}FeO_2^+$) *m*/*z* 294.03377). ^{1}H NMR ($CDCl_3$): δ 6.85 (d, J_{HH} 9 Hz, $C_6H_3(OH)_2$, 1 H), 6.78 (d, J_{HH} 3 Hz, $C_6H_3(OH)_2$, 1 H), 6.72 (dd, J_{HH} 3, 9 Hz, $C_6H_3(OH)_2$, 1H), 4.52 (t, J_{HH} 2 Hz, C_5H_4, 2 H), 4.39 (t, J_{HH} 2 Hz, C_5H_4, 2 H), 4.22 (s, C_5H_4, 5 H). LR-MS: 295 (M$^+$ + 1, 18), 294 (M$^+$, 80), 293 (M$^+$ − H, 5), 292 (M$^+$ − 2H, 10), 228 (M$^+$ − C_5H_5), 100). IR (Nujol (cm^{-1})): 3319 (s), 1626 (w), 1510 (s), 1242 (w), 1196 (vs), 1127 (w), 1108 (m), 1073 (w), 1043 (w), 1020 (w), 1004 (m), 933 (w), 846 (m), 818 (s), 782 (s), 726 (m), 497 (s).

(29) (a) Allgeier, A. M.; Slone, C. S.; Mirkin, C. A.; Liable-Sands, L. M.; Yap, G. P. A.; Rheingold, A. L. *J. Am. Chem. Soc*. **1997**, *119*, 550−559. (b) Pierpont, C. G. *Coord. Chem. Rev.* **2001**, *216*, 99−125. (c) Dei, A.; Gatteschi, D.; Sangregorio, C.; Sorace, L. *Acc. Chem. Res.* **2004**, *37*, 827−835.

(30) (a) Rice, C. R.; Ward, M. D.; Nazeeruddin, N. K.; Grätzel, M. *New J. Chem.* **2000**, *24*, 651−652. (b) Lucas, N. T.; McDonagh, A. M.; Hook, J. M.; Colbran, S. B. *Eur. J. Inorg. Chem.* **2005**, 496−503. (c) Lucas, N. T.; McDonagh, A. M.; Dance, I. G.; Craig, D. C.; Colbran, S. B. *Dalton Trans.* **2006**, 680−685.

(31) He, Z. C.; Colbran, S. B.; Craig, D. C. *Chem. Eur. J.* **2003**, *9*, 116−129.

Fc−q (3). Boron tribromide (5.9 mL, 62 mmol) was added to a solution of **1** (4.0 g, 12 mmol) in dichloromethane (60 mL) cooled in an acetone/dry ice bath. The resulting dark red solution was allowed to warm to room temperature and stirred overnight. The solvent was removed in vacuo and the residue cooled in an ice bath. Methanol (30 mL) was added via cannula followed by saturated aqueous sodium carbonate (30 mL). The mixture was extracted quickly in air with dichloromethane (3 × 50 mL), and the combined organic extracts were combined and dried over anhydrous magnesium sulfate. The solvent was removed, and the resulting solid was dissolved in dichloromethane (40 mL). 2,3-Dichloro-5,6-dicyano-1,4-benzoquinone (2.26 g, 10 mmol) was added, whereupon the solution immediately changed from orange to green. The solution was filtered and the solvent removed in vacuo to give a green solid. The product was purified by thin-layer chromatography with dichloromethane as eluant. Subsequent recrystallization of the green band from hexane gave 2.10 g (57%) of **3** as dark green crystals. Anal. Found: C 65.15, H 4.41. Calc: C 65.78, H 4.14. Mp: 128−130 °C. ^{1}H NMR ($CDCl_3$): δ 6.81 (d, J_{HH} 3 Hz, $C_6H_3O_2$, 1 H), 6.70 (d, J_{HH} 8 Hz, $C_6H_3O_2$,1 H), 6.65 (dd, J_{HH} 3, 8 Hz, $C_6H_3O_2$, 1H), 4.90 (t, J_{HH} 2 Hz, C_5H_4, 2 H), 4.57 (t, J_{HH} 2 Hz, C_5H_4, 2 H), 4.09 (s, C_5H_4, 5 H). ^{13}C NMR ($CDCl_3$): δ 186.4, 185.9, 148.5, 137.2, 136.3, 126.7, 75.9, 72.4, 69.7, 70.6. LR-MS: 293 ($M^+ + 1$, 20), 292 (M^+, 100), 226 ($M^+ - C_5H_5$, 75). IR (Nujol (cm^{-1})): 3058 (w), 1671 (s), 1647 (vs), 1615 (s), 1579 (vs), 1353 (w), 1329 (m), 1290 (vs), 1271 (m), 1109 (m), 1062 (m), 1039 (w), 985 (w), 917 (m), 904 (w), 839 (m), 826 (m), 502 (m), 487 (w), 431 (m).

Fc−catMe$_2$ (4). The diazonium salt of 1,2-dimethoxyaniline was prepared by the slow addition of sodium nitrite (83 mg, 1.2 mmol) to a stirred solution of 1,2-dimethoxyaniline (180 mg, 1.17 mmol) in aqueous sulfuric acid (0.2 M). The resultant solution was added rapidly to ferrocene (270 mg, 1.17 mmol) dissolved in glacial acetic acid (10 mL) under an inert atmosphere. The resulting green-brown solution was stirred overnight at room temperature and then poured into water. The mixture was extracted with dichloromethane (3 × 20 mL), the combined organic extracts were treated with aqueous sodium carbonate until neutral and dried over magnesium sulfate, and the solvent was removed. The crude product was recrystallized from dichloromethane/methanol to yield 65 mg (14%) of **4** as an orange solid. Anal. Found: C 67.22, H 5.66. Calc: C 67.10, H 5.66. ^{1}H NMR ($CDCl_3$): δ 7.14 (s, C_6H_3, 1H), 7.07 (d, J_{HH} 9 Hz, C_6H_3, 1 H), 6.81 (d, J_{HH} 8 Hz, C_6H_3,1 H), 4.57 (s, C_5H_4, 2 H), 4.27 (s, C_5H_4, 2 H), 4.05 (s, C_5H_4, 5 H). LR-MS: 323 ($M^+ + 1$, 23%), 322 (M^+, 100), 307 ($M^+ - CH_3$, 10). IR (KBr pellet (cm^{-1})): 3087 (w), 3004 (w), 2956 (m), 2931 (m), 2833 (m), 1639 (vs), 1584 (vs), 1523 (s), 1506 (m), 1486 (m), 1472 (m), 1439 (s), 1268 (w), 1247 (vs), 1218 (s), 1206 (w), 1172 (vs), 1140 (vs), 1026 (vs), 815 (vs), 755 (m), 740 (m).

Fc−catH$_2$ (5). Boron tribromide (0.35 mL, 2.8 mmol) was added to a solution of **4**[14] (609 mg, 1.89 mmol) in dichloromethane (30 mL) cooled to −78 °C in an acetone/dry ice bath. The resulting solution was stirred for 30 min at −78 °C and then for another 30 min at room temperature. The reaction was quenched by the cautious addition of methanol. The solution was extracted with aqueous sodium thiosulfate and then with water and dried over magnesium sulfate, and the solvent was removed in vacuo. The residue was treated with methanol, whereupon an orange impurity precipitated. The mixture was filtered, and the filtrate was reduced in volume in vacuo to give 393 mg (75%) of **5** as an orange-brown solid. The product is unstable in air and decomposes over time. Anal. Found: C 64.26, H 4.99. Calc: C 65.34, H 4.99. ^{1}H NMR (d_6-acetone): δ 7.69 (s, OH, 1 H), 7.67 (s, OH, 1H), 6.97 (s, C_6H_3, 1 H), 6.82 (d, J_{HH} 8 Hz, C_6H_3,1 H), 6.74 (d, J_{HH} 8 Hz, C_6H_3, 1H), 4.66 (s, C_5H_4, 2 H), 4.31 (s, C_5H_4, 2 H), 4.06 (s, C_5H_4, 5 H). ^{13}C NMR (d_6-acetone): δ 205.2, 120.1, 117.8, 114.9, 113.3, 69.8, 68.5, 65.9. LR-MS: 295 ($M^+ + 1$, 5%), 294 (M^+, 17), 292 ($M^+ - 2H$, 5). IR (KBr pellet (cm^{-1})): 3345 (vs), 3090 (w), 1604 (s), 1539 (s), 1468 (s), 1444 (s), 1387 (s), 1362 (w), 1296 (s), 1259 (s), 1207 (w), 1185 (w), 1104 (s), 1015 (w), 809 (s), 778 (m).

Acknowledgment. This research was supported by the Australian Research Council (Grant: DPO557462) and The University of New South Wales.

Supporting Information Available: A figure showing the solvent dependence of the lowest energy visible band for **3**. This material is available free of charge via the Internet at http://pubs.acs.org.

OM060040X